High pressure methane catalytic combustion over novel partially coated $LaMnO_3$-based monoliths

Paola Sabrina Barbato[1], Valeria Di Sarli[1], Gianluca Landi*[1] and Almerinda Di Benedetto[2]

[1] *Institute for Researches on Combustion-CNR, P.le Tecchio 80, 80125 Naples, Italy*

[2] *Department of Chemical, Materials and Industrial Processes Engineering (DICMAPI) – University of Naples Federico II, P.le Tecchio 80, 80125 Naples, Italy*

**corresponding author: landi@irc.cnr.it*

Abstract

This work is focused on the experimental validation of a novel partially coated "core-shell" monolith configuration proposed for high pressure (up to 10 bar) methane combustion under self-sustained conditions. In particular, perovskite-based catalyst is deposited onto the walls of the outer channels, core zone being uncoated. The effect of pressure on ignition and quenching is studied for two partially coated monoliths with different coating degree, while a fully coated monolith is used as reference. Results show that coating only the external channels is an effective strategy to activate homogeneous reaction in the whole monolith. Moreover, independently from coating degree, ignition pressure, fuel conversion and flow rate a single value for developed thermal power is obtained at ignition conditions. This result suggests that ignition occurrence is more related to global more than local heat balance.

Keywords: *Methane; Catalytic Combustion; Perovskite; Partially Coated Monolith.*

1. INTRODUCTION

Catalytic combustion (CC) has been proposed as an alternative route to produce energy in an environmental-friendly and safe manner [1-3]. Despite the great interest and the huge number of literature papers devoted to CC, its commercial application is mainly limited to pollution abatement, like TWCs. Moreover, typical features of catalytic structured systems generally cannot satisfy all process requirements and, consequently, complex process designs have been proposed for power and heat generation by catalytic combustion [4]. As a matter of fact, only few commercial catalytic burners have been proposed for gas turbine systems [5, 6]. Such systems are able to reduce NO_x emissions into the sub-9 ppm range [5-7].

A suitable catalyst should exhibit several features due to the different needs of the combustion process. In particular, low ignition temperatures, possibly close to the compressor outlet temperature (290-450°C depending on load), are required and, as a consequence, catalyst should have high activity at low temperatures. On the other hand, a catalytic combustion process is carried out at relatively high temperature (at least 900-1000°C), but the turbine inlet temperature is even higher, thus catalyst should be stable under these temperature conditions. Moreover, mechanical resistance is required due to the stresses related to the high velocities of the gas flow through the catalyst. Starting from the latter issue, the use of structured catalyst, i.e. ceramic or metallic honeycombs coated with thin layers of active phase, allows to prepare catalytic systems that exhibit not only high mechanical properties but also very low pressure drops and high surface-to-volume ratios.

The good activity at low temperature has pushed towards the use of noble metal catalysts, but their application is limited due to their high cost and tendency to volatilize and/or sinter and/or deactivate at relatively high temperatures [2,8,9]. These limitations could be partially overcome by using cheaper and more thermally resistant catalysts such as perovskites [10]. Among perovskites, $LaMnO_3$ is one of the most active formulations for methane total oxidation [11]. Perovskites exhibit low surface areas, thus limiting the specific activity. Nevertheless, $LaMnO_3$ supported on La-

stabilized γ-Al_2O_3 showed not only good performance towards combustion of different fuels and fuel blends [12-17], but also quite stable structural properties, as evidenced by small reduction of the specific surface area [18].

Despite the great interest in power generation applications, the literature works on catalytic combustion under pressure remain limited [12-17, 19-23] and mainly devoted to noble metals [19-23]. Even at moderate pressure (up to 5 bar), the heterogeneous and homogeneous pathways are coupled [24] and the pressure effect on homogeneous reaction is fuel-specific [25-27]. In order to obtain high inlet temperature to the turbine, staged combustion, generally coupled to a post-catalytic flame stage, has been studied [28-29]. In these cases, the complete fuel consumption has been obtained by coupling heterogeneous and homogeneous combustion in different sections of the burner. According to our previous works, the occurrence of homogeneous reactions is not only unavoidable but also sustains the combustion process and allows to overcome mass transfer limitations, generally occurring within monolithic reactors [17]. As a consequence, the novel idea we proposed [16] was to burn methane in a partially coated monolith, catalyst being deposited only onto the external channels (core-shell configuration). We checked the behavior of this novel configuration by developing a multichannel CFD model. Simulation results allowed us to identify an optimal reactor configuration in which heterogeneous reaction is activated in the external coated channels (with a minimum coating corresponding to 40% of channels) and is responsible for the temperature increase and, thus, for the on-set of homogeneous reaction both in the coated and uncoated channels [16]. In the work presented in this paper, we first prepared “core-shell” partially coated monoliths and then conducted an experimental campaign in order to test the performance of this novel configuration during methane combustion under self-sustained conditions and pressure up to 10 bar.

2. EXPERIMENTAL

2.1 Monolith Preparation

In this work, monoliths with different coating fractions were tested. In particular, a fully coated, as reference, and two partially coated "core-shell" samples were prepared, the features of which being reported in Table 1. The "core-shell" monoliths were obtained by creating a parallelepiped hole with square section in a monolith previously cut as a cylinder (see Figure 1a and 1c (middle)). The catalyst was deposited onto the surface of the hollow monolith by the procedure described below. A non-coated monolith was cut with square section and size corresponding to the hole (Figure 1a) and then inserted in order to occupy the void volume of the coated part (Figure 1b). The reference system, i.e. the fully coated sample, was obtained by simply cutting a monolith as a cylinder without creating the hole. 20%$LaMnO_3$/La-stabilized γ-Al_2O_3 was deposited as active phase onto the walls of the catalytic parts.

The active phase was deposited by means of a modified dip coating procedure as reported elsewhere [16]. Briefly, a thin layer of γ-Al_2O_3 washcoat was first deposited by dipping the monoliths in an aqueous slurry of ball milled high surface area alumina (CK 300), bohemite (Disperal, CONDEA) and nitric acid. The excess slurry was flushed away by air flow and then the sample was dried in a stove at 120°C and calcined at 550°C. These operations were repeated several times in order to achieve the target of 40% wt/wt of the washcoat. A final calcination was then performed at 800°C. Subsequently, an aqueous solution of $La(NO_3)_3$ first and another one of $La(NO_3)_3$ and $Mn(CH_3COO)_2 \cdot 4H_2O$ were used respectively for stabilization of alumina with 5% La_2O_3 and impregnation of the $LaMnO_3$ active phase with similar procedure of drying and calcination (800°C). Two examples of fully coated monolith are reported in Figure 1c, while in Figure 1b a hollow coated monolith with the uncoated insertion is shown.

2.2 Experimental Setup

The fully or partially coated monoliths were stacked between two mullite foams (acting as radiation shield) and wrapped in ceramic wool before being inserted in the stainless steel housing (d_e = 25.4 mm, L = 70 mm) as depicted in Figure 2. As shown in Figure 2, 6 thermocouples, sealed with Multiple-Hole Ceramic gland feedthroughs (Conax Technologies, MHC series), were used to measure the axial profile of the whole reactor including the monolithic section. In particular, three thermocouples provided the temperature measurements inside the monoliths and were positioned at 5 mm from the inlet of the monolith (T_3), at the middle (T_4) and at 5 mm to the end of the monolith (T_5) in the central channel. It should be noted that the central channel is coated for F and uncoated for P1 and P2 monoliths.

Combustion tests were carried out in a lab-scale experimental rig designed to work at pressures up to 12 bar and described in more details in [17]. The analysis system (ABB AO2000) is equipped with four modules for the online and continuous analysis of the main gas species (CH_4, CO_2, and CO by infrared detectors; O_2 by a paramagnetic detector) and with a cross-sensitivity correction.

Experiments were conducted at constant pre-heating temperature. Operating pressure was increased from approximately 1 to 12 bar. The mass flow rate was kept constant (i.e., the volumetric flow rate decreased with increasing pressure). The conditions adopted are summarized in Table 2. Some tests were repeated and gave results that differ within the experimental error.

3. RESULTS

3.1 Monolith performances

In Figure 3, the steady state methane conversion is plotted as a function of pressure for F (▲), P1 (●) and P2 (■) monoliths. Experiments were carried out by increasing (full symbols) and then decreasing (empty symbols) the pressure in the range of 1-8 bar. The behavior of the fully coated monolith has been studied in previous works [16-17] and is here reported as reference (black triangles in Figure 3).

With all monoliths, it is found that, as the operating pressure increases, the methane conversion slightly increases up to reach the ignition conditions. The ignition pressure is equal to 3 atm in the fully coated (F) monolith, 4 atm in P1 monolith and 5 atm in P2 monolith.

After ignition has been obtained, a jump to the ignited branch is found. In F and P1 monoliths, a complete methane conversion is reached, while in P2 monolith the maximum conversion is equal to about 80 %. In F and P1 configurations, as the operating pressure decreases along the ignited branch, the methane conversion remains high even at low pressures (hysteresis behavior), suggesting the presence of steady state multiplicity. In P2 configuration, as the operating pressure decreases along the ignited branch (starting from P = 8 atm), the methane conversion decreases and reaction extinguishes at a pressure slightly lower than the ignition one (P = 4.5 atm).

It is worth noting that the methane conversion over the ignited branch remains constant with increasing (full symbols) and decreasing (empty symbols) pressure only for F and P1 configurations. In P2 configuration, over the ignited branch the methane conversion is the same only at P = 8 atm. At lower pressure, the methane conversion is higher when starting from P = 8 atm and lower when starting from pressure lower than the ignition pressure. This different behavior can be attributed to the activation of the homogeneous reaction in all channels. When starting at low pressure (i.e. P = 3 atm), the channel temperatures are low. When ignition takes place, the activation of catalytic and homogeneous reaction allows increase of temperature in the channels. However, the methane conversion is not complete, suggesting that in some uncoated channels the homogeneous reaction is not activated since the heat produced by combustion in the coated channels is not enough to heat up the uncoated channels. Conversely, when starting from an already ignited steady state (P = 8 bar), the channel temperatures are high enough to sustain the activation of homogeneous reaction and then higher methane conversions are attained.

In Figure 3, the methane conversion attainable only with the coated channels of each configuration is also plotted (– for P1, -- for P2). For P1 configuration, this value corresponds to 79 %, while for P2 configuration it is equal to 63 %. In both configurations, when the ignition pressure is reached,

the methane conversion becomes higher than these values, suggesting that the homogeneous reaction is surely activated also in some or all of the uncoated channels.

In Figure 4, the temperature profiles measured along the axial direction are shown for the three configurations (F, P1 and P2), at different pressures under not ignited conditions.

Temperatures are measured inside the central channels of the monoliths. As a consequence, temperatures for P1 and P2 configurations are related to the uncoated section of the monolithic reactor.

The temperature levels inside the central channel of the monolith are higher in the fully coated configuration. At the ignition pressure, about the same methane conversion is attained for all configurations (Figure 3). A significant difference is found in terms of temperature. Indeed, in the fully coated configuration, the temperature is higher than in P1 and P2 configurations. This result has to be attributed to the fact that, under these conditions, the channels surrounding the central channel are uncoated in P1 and P2 configurations and then are not ignited.

The temperature profiles obtained at steady state conditions over the ignited branch are plotted in Figure 5 at different pressures as measured in the central channels of all configurations.

Temperatures are measured only in three positions inside the central channel. As a consequence, from these values, it is not possible to draw the complete temperature spatial profile. However, these measurements may give an idea of the position and of the movement of the reaction front along the axial direction in the channel.

In F configuration, it appears that, as the operating pressure increases on the ignited branch, the maximum temperature is positioned at the same location, close to the inlet. As the operating pressure decreases on the ignited branch (methane conversion is still complete), the maximum temperature shifts downstream. From our measurements, at P = 2 bar, it is not possible to visualize the position of the front, while at P = 1 atm, the front is found at ~ 40 mm.

In P1 configuration, as the operating pressure increases on the ignited branch, the maximum temperature seems to increase, but actually it is hiding a movement of the reaction front upstream.

As the operating pressure decreases on the ignited branch (from 8 to 3 and 2 bar), the reaction front seems to move downstream.

At pressures higher than the ignition pressure in both F and P1 configurations, a complete methane conversion is attained. As a consequence, all channels are ignited. The temperature level in F configuration is higher than in P1 configuration. This result may suggest that in P1 configuration the reaction front is positioned downstream with respect to F configuration.

In P2 configuration, the methane conversion is not complete even over the ignited branch (Figure 3) and accordingly the temperature levels are significantly lower than those reached in F and P1 configurations.

3.2 Effect of flow rate

The role of the flow rate was previously studied in the fully coated configuration [16] and by means of a CFD model in the partially coated configurations [17]. As the flow rate is increased, the methane conversion is affected by two co-current phenomena: increasing the flow rate means decreasing the residence time but increasing the thermal power.

In Figure 6, the methane conversion is plotted as a function of pressure as obtained for all the configurations investigated at different flow rates (30, 45, 60 and 86 slph). The maximum theoretical methane conversions attainable in the monolith when only the coated channels are ignited are also shown in the plots (— for P1, -- for P2).

At the lowest value of the flow rate (Q = 30 slph), in all the configurations, the methane conversion is not complete. In F and P1 configurations, at high pressures, the same conversion is attained. In P1 configuration, the methane conversion is also higher than the full methane conversion reached when only the coated channels are ignited (—), suggesting that homogeneous reaction is activated also in the uncoated channels. Conversely, in P2 configuration, the homogeneous reaction is not activated in the uncoated channels, being the methane conversion lower or equal to the maximum conversion in the coated channels (– –). In these conditions, the thermal power is too low with respect to the heat losses to allow ignition and/or the reached temperature is not high enough for the onset of the

homogeneous reaction.

When increasing the flow rate (b and c), in F and P1 configurations, full conversion is attained and in P2 configuration some uncoated channels are ignited, being the methane conversion higher than the coated channel theoretical conversion (--).

At the highest flow rates investigated, (Q= 60 and 86 slph), on decreasing the pressure down to P= 1 atm, no extinction is observed being the thermal power high enough to overcome the heat losses. Conversely, in P2 configuration, on increasing the flow rate (Q= 86 slph), ignition does not occur anymore since the residence time is too low to allow ignition of the catalytic reaction.

In Figures 7 and 8, the temperature profiles measured in the central channel are shown at all the flow rates investigated under not ignited and ignited conditions, respectively.

On the lower branch corresponding to the not ignited conditions, the reaction rate is controlled by the catalytic reaction and then it is highly sensitive to the residence time. Accordingly, by increasing the flow rate, the maximum temperature shifts towards the exit of the monoliths due to the decreased residence time. It is worth noting that on increasing the flow rate, for all configurations, the effect of pressure on the temperature profiles decreases. On the ignited branches, the temperature profiles are quite affected by the flow rates.

At 30 splh, measured temperatures do not exceed 700°C. Even if the actual maximum temperature could not be detected, if positioned between two measurement points, the mean temperature seems not high enough to allow a vigorous homogeneous reaction rate, thus explaining the incomplete conversion. For P1 monolith, temperature profiles reveal the presence of a reaction front close to the entrance of the monolith, as it occurs for F monolith (Figure 8).

It is noteworthy that, in the case of P1, T_3 (i.e. the temperature at 5 mm from the monolith entrance) and T_4 (i.e. the temperature at 5 mm from the monolith entrance) are lower and higher respectively than the corresponding temperatures measured inside F monolith. These evidences suggest that the reaction front of the homogeneous reactions is located downstream in P1 with respect to F monolith, as found by CFD simulations reported in [16].

The temperature profiles for P2 configuration reveal that the temperatures measured inside P2 monolith are lower than the corresponding temperatures detected inside F and P1 monoliths. This suggests that homogeneous reaction rate, strongly depending on the temperature, is lower and, consequently, a fraction of the fuel cannot be converted. By decreasing the pressure, the maximum temperature shifts downstream.

3.3 Thermal power

In Figure 9, the thermal power (P) is shown as a function of the operating pressure for the three monoliths. The thermal power is calculated according to following equation:

$$\dot{P} = \dot{n}_{CH_4} . \Delta H^{c}_{CH_4} . x_{CH_4} \quad (1)$$

where $\dot{n}_{\mathrm{CH_4}}$ is methane flow rate (mol/s), $\Delta H^{c}_{CH_4}$ is the heat of combustion of methane (J/mol) and x_{CH_4} is the steady state methane conversion.

From the plots of Figure 9, regardless of the flow rate and/or the coating degree, a unique threshold value of P between non ignited and ignited conditions can be identified corresponding to 5 W (dotted lines in Figures 9). We already obtained similar results by varying the fuel composition at fixed flow rate [15] and the flow rate at fixed fuel composition [16] over a fully coated monolith. In particular, we found the threshold values as equal to 6.3 W [15] and 3.7 W [16]. The different value here obtained has to be attributed to the different size of the reactors or, better, to the different surface to volume ratio.

In those works [15-16], we stated that this behavior could be explained by considering that in order to fully ignite the system, it was necessary to reach a certain temperature. The present results show that even in the partially coated monolith the same threshold value is reached, thus providing new insights into this behavior.

By changing the flow rate and the catalyst coating degree, the temperatures reached in the different monoliths at ignition are different (Figures 4), thus suggesting that the local temperature is not the key parameter to get ignition in the whole monolith.

On the other hand, the constant value of the developed thermal power needed to obtain ignition suggests that the strict condition for getting ignition is that the heat produced by reaction is higher than the heat losses. The value of P = 5 W is then related to the entity of heat losses of the lab equipment. By reducing heat losses, the critical value of P is expected to be reduced and the ignition region is expected to become wider.

In P2 configuration, ignition is not obtained at the highest flow rate investigated (86 slph) and accordingly the thermal power is lower than 5 W even at 9 bar.

In all the configurations investigated, at flow rate equal to 30 slph (Figure 9), when the thermal power reaches the threshold value (5 W), ignition is observed, but partial methane conversion is attained (lower than 100 %). This result suggests that at this value of the flow rate, the catalytic reaction is ignited while the homogeneous reaction may be not active. The activation of the homogeneous reaction is significantly sensitive to temperature.

As a result we may affirm that ignition in catalytic combustors is not allowed by local hot-spots with temperature higher than the ignition temperature. In order to allow ignition, the reaction front has to be sustained and this is possible only when globally the heat produced by reaction (thermal power) overcomes the heat losses.

Conversely, since the activation of the homogeneous reaction is a required step for a complete fuel conversion [16-17], after the stabilization of the catalytic reaction a complete conversion is reached only when the temperature level inside the channels is sufficiently high to activate the homogeneous reaction.

3.4 Effect of pre-heating temperature

P2 configuration is not ignited at the highest flow rate investigated (Q = 86 slph). We performed tests at a higher pre-heating temperature (545 °C) in order to find the conditions of ignition of the less coated configuration. From the operative point of view, we increased the pre-heating temperature at fixed pressure (P = 9 bar). When measured conversion was about 18%, corresponding to about 5 W developed power, ignition occurred and conversion reached 93%.

This value, even if lower than 1, is higher than those reported in Figure 6 for P2 under ignited conditions, confirming that on this partially coated monolith fuel conversion limitation is mainly due to the thermal balance causing relatively low temperatures inside the uncoated section.

In Figure 10, steady state conversions (a) and temperature profiles (b) obtained by decreasing the operating pressure from 9 to 1 bar are reported. Conversion slightly decreases by decreasing the pressure but remains higher than the value corresponding to complete conversion within the catalytic section (horizontal dashed line in Figure 10), suggesting that a part of the homogeneous reaction occurring within the uncoated section is carried on in the last section of the monolith. At the same time, the maximum temperature shifts downstream, as expected. At 2 bar, quenching is detected and temperatures fall down.

3.5 Operating maps

The previously obtained results show the key role of pressure and flow rate in affecting the ignition/extinction behavior of the monoliths.

In Figure 11, the operating maps of F (▲), P1 (●) and P2 (■) monoliths are shown as obtained by rearranging all the results obtained. Three zones are identified: ignited zone, steady-state multiplicity zone and not ignited zone.

Quenching pressure line is obtained only for partially coated monolith at low flow rates under the experimental conditions here investigated. The decrease of quenching pressure by increasing the flow rate suggests that the quenching mechanism is extinction, as expected at low flow rates [16].

The ignited region, the most important for applicative purposes, reduces by reducing the catalyst amount. This confirms our previous results suggesting that catalyst not only plays a major role for fuel ignition but also contributes to stabilize the reaction front under ignited conditions [17].

Nevertheless, it is noteworthy that the above considerations are qualitatively valid for any size of the monolithic reactor but the values of the stability map are significantly affected by the reactor size, as it can be highlighted by comparing present results to our previous ones [17]. With larger reactors, showing a higher adiabaticity degree, the heat losses are a lower fraction of the produced

heat, with a consequent beneficial effect on the thermal profiles of the monolith. So, in this case, the use of partially coated monoliths would be preferable, because of their lower cost (due to the reduced catalyst amount), without a performance reduction. As a matter of fact, we have demonstrated that also at our lab scale it is possible to obtain a complete fuel conversion on a partially coated monolith. On the other hand, at small scales, as those of micro-combustors, heat losses cannot be neglected and thus a more stable system would be preferable, i.e. a fully coated or a partially coated monolith with a high coating degree (as P1 configuration).

4. CONCLUSIONS

The performances of three differently coated monoliths have been compared: a fully coated monolith (configuration F), a monolith in which only 79 % of the channels are coated (configuration P1) and a monolith in which only 63 % of the channels are coated (configuration P2). The monoliths were tested at different pressures and flow rates. Results show that configuration P1 behaves similarly to configuration F, while configuration P2 has a very narrow range of operability never reaching a complete methane conversion regime. However, in the case of P2 configuration, the methane conversion is higher than the theoretical methane conversion that is reached when only the coated channels are ignited. This result suggests that, also in this case, the homogeneous reaction is activated inside the uncoated channels. However, since the methane conversion is not complete, in some uncoated channels the heat transferred is not enough to sustain the homogenous reaction.

The key role of the thermal power has been highlighted showing that to ensure activation of the reaction in all channels a threshold value of the thermal power has to be reached. This value is similar for all configurations (F, P1 and P2) and is equal to 5 W.

The thermal power has to overcome heat losses towards the external environment, trapping heat inside the uncoated channels thus allowing reactions to sustain. Once ignition has occurred, in order

to get the full methane conversion, local temperature should be high enough to activate the homogeneous reaction in the uncoated channels.

ACKNOWLEDGEMENT

This work was financially supported by MiSE-CNR "CO_2 capture- Carbone pulito" Project (Italy).

REFERENCES

1. J.H. Lee, D.L. Trimm, Catalytic combustion of methane, Fuel Process. Technol. 42 (1995) 339-359.
2. D. Ciuparu, M.R. Lyubovsky, E. Altman, L.D. Pfefferle, A. Datye, Catalytic combustion of methane over palladium-based catalysts. *Catal. Rev. 44 (***2002)** 593-649.
3. P.S. Barbato, G. Landi, New concepts for power production by catalytic combustion: a short review, *Curr. Top. Catal. 10 (***2012)** 75-92.
4. T. Furuya, K. Sasaki, Y. Hanakata, T. Ohhashi, M. Yamada, T. Tsuchiya, Y. Furuse, Development of a hybrid catalytic combustor for a 1300°C class gas turbine, Catal. Today 26 (1995) 345-350.
5. S. Cocchi, G. Nutini, M. J. Spencer, S. G. Nickolas, Catalytic combustion system for a 10 MW class power generation gas turbine, Catal. Today 117 (2006) 419- 426.
6. H. Karim, K. Lyle, S. Etemad, L.L. Smith, W.C. Pfefferle, P. Dutta, K. Smith, Advanced catalytic pilot for low NOx industrial gas turbines, J Eng Gas Turbines Power 125 (2003) 879-884.
7. V. Di Sarli, Stability and emissions of a lean pre-mixed combustor with rich catalytic/lean-burn pilot, Int. J. Chem. React. Eng. 12 (2014) 1-13.
8. G. Groppi, W. Ibashi, E. Tronconi, P. Forzatti, Structured reactors for kinetic measurements under severe conditions in catalytic combustion over palladium supported systems, Catal. Today 69(1-4) (2001) 399-408.

9. J.G. McCarty, M. Gusman, D.M. Lowe, D.L. Hildenbrand, K.N. Lau, Stability of supported metal and supported metal oxide combustion catalysts, Catal. Today 47 (1999) 5-17.
10. T.V. Choudhary, S. Banerjee, V.R. Choudhary, Catalysts for combustion of methane and lower alkanes, Appl. Catal. A: Gen. 234 (2002) 1-23.
11. G. Saracco, F. Geobaldo, G. Baldi, Methane combustion on Mg-doped $LaMnO_3$ perovskite catalysts, Appl. Catal. B: Environ 20 (1999) 277-288.
12. A. Di Benedetto, P.S. Barbato, G. Landi, Effect of CO_2 on the Methane Combustion over a Perovskyte Catalyst at High Pressure, Energ Fuel 27 (2013) 6017-6023 DOI: 10.1021/ef401818z
13. P.S. Barbato, A. Di Benedetto, V. Di Sarli, Gianluca Landi, Ignition and Quenching Behaviour of High Pressure CH_4 Catalytic Combustion over a $LaMnO_3$ Honeycomb, Chem. Eng. Trans. 32 (2013) 655-660 DOI:10.3303/CET1332110
14. G. Landi, P.S. Barbato, A. Di Benedetto, R. Pirone, G. Russo, High pressure kinetics of CH_4, CO and H_2 combustion over $LaMnO_3$ catalyst, Appl. Catal. B: Environ. 134-135 (2013) 110-122 DOI: 10.1016/j.apcatb.2012.12.040
15. P.S. Barbato, G. Landi, G. Russo, Catalytic combustion of CH_4-H_2-CO mixtures at pressure up to 10 bar, Fuel Proc. Technol. 107 (2013) 147-154 DOI: 10.1016/j.fuproc.2012.08.024
16. A. Di Benedetto, G. Landi, V. Di Sarli, P.S. Barbato, R. Pirone, G. Russo, Methane catalytic combustion under pressure, Catal. Today 197 (1) (2012) 206-213 DOI: 10.1016/j.cattod.2012.08.032
17. P.S. Barbato, A. Di Benedetto, V. Di Sarli, G. Landi, R. Pirone, High-Pressure Methane Combustion over a Perovskyte Catalyst, Ind. Eng. Chem. Res. 51 (22) (2012) 7547-7558 DOI: 10.1021/ie201736p
18. S. Cimino, L. Lisi, R. Pirone, G. Russo, M. Turco, Methane combustion on perovskites-based structured catalysts, Catal. Today 59 (2000) 19-31.

19. M. Reinke, J. Mantzaras, R. Schaeren, R. Bombach, A. Inaunen, S. Schenker, High-pressure catalytic combustion of methane over platinum: In situ experiments and detailed numerical predictions, Combust. Flame 136 (2004) 217-240.
20. K. Persson, A. Ersson, A. Manrique Carrera, J. Jayasuriya, R. Fakhrai, T. Fransson, S. Jaras, Supported palladium-platinum catalyst for methane combustion at high pressure, Catal. Today 100 (2005) 479-483.
21. M. Reinke, J. Mantzaras, R. Bombach, S. Schenker, A. Inaunen, Gas phase chemistry in catalytic combustion of methane/air mixtures over platinum at pressures of 1 to 16 bar, Combust. Flame 141 (2005) 448-468.
22. J. C. G. Andrae, D. Johansson, M. Bursell, R. Fakhrai, J. Jayasuriya, A. Manrique Carrera, High-pressure catalytic combustion of gasified biomass in a hybrid combustor, Appl. Catal. A: Gen. 293 (2005) 129-136.
23. K. Persson, L. D. Pfefferle, W. Schwartz, A. Ersson, S. G. Jaras, Stability of palladium-based catalysts during catalytic combustion of methane: The influence of water, Appl. Catal. B: Environ. 74 (2007) 242-250.
24. S. Karagiannidis, J. Mantzaras, K. Boulouchos, Stability of hetero-/homogeneous combustion in propane- and methane-fueled catalytic microreactors: Channel confinement and molecular transport effects, P. Combust. Inst. 33 (2) (2011) 3241-3249.
25. J. Mantzaras, Catalytic Combustion of Syngas, Comb. Sci. Tech. 180 (2008) 1137-1168.
26. J. Mantzaras, Catalytic combustion of syngas, in T.C. Lieuwen, V. Yang, R. Yetter (Eds.), Synthesis Gas Combustion, CRC Press (Taylor & Francis Group), Boca Raton, 2010, pp. 223-260.
27. J. Mantzaras, R. Bombach, R. Schaeren, Hetero-/homogeneous combustion of hydrogen/air mixtures over platinum at pressures up to 10 bar, P. Combust. Inst. 32 (II) (2009) 1937-1945.

28. K.W. Beebe, K.D. Cairns, V.K. Pareek, S.G. Nickolas, J.C. Schlatter, T. Tsuchiya, Development of catalytic combustion technology for single-digit emissions from industrial gas turbines, Catal. Today 59(1–2) (2000) 95–115.
29. R. Carroni, V. Schmidt, T. Griffin, Catalytic combustion for power generation, Catal. Today 75 (1–4) (2002) 287–295.

Figures captions

Figure 1 - Some pictures of the uncoated and coated monoliths.

Figure 2 - Schematic drawing of the reactor configuration with positioning of the thermocouples.

Figure 3 - Methane conversion as a function of pressure for F (▲), P1 (●) and P2 (■) monoliths. Flow rate = 45 slph. Tests have been performed by increasing (full symbols) and then by decreasing (empty symbols) pressure.

Figure 4 - Spatial temperature profiles measured under not ignited conditions for F, P1 and P2 monoliths at different pressures. Flow rate = 45 slph.

Figure 5 - Spatial temperature profiles measured under ignited conditions for F, P1 and P2 monoliths at different pressures. Flow rate = 45 slph. Tests have been performed after ignition by increasing (full symbols) and then by decreasing (empty symbols) the pressure.

Figure 6 - Methane conversion as a function of operating pressure for F (▲), P1 (●) and P2 (■) monoliths at different flow rates: 30 (a), 45 (b), 60 (c) and 86 (d) slph. Tests have been performed by increasing (full symbols) and then by decreasing (empty symbols) the pressure.

Figure 7 - Spatial temperature profiles measured under not ignited conditions for F, P1 and P2 monoliths at different pressures and flow rates.

Figure 8 - Spatial temperature profiles measured under ignited conditions for F, P1 and P2 monoliths at different pressures and flow rates. Tests have been performed after ignition by increasing (full symbols) and then by decreasing (empty symbols) the pressure.

Figure 9 - Thermal power as a function of pressure for F (▲), P1 (●) and P2 (■) monoliths at different flow rate: 30 (a), 45 (b), 60 (c) and 86 (d) slph. Tests have been performed by increasing (full symbols) and then by decreasing (empty symbols) the pressure.

Figure 10 - Methane conversion (a) and temperature profiles (b) measured under ignited conditions for P2 monolith at different pressures, Q = 86 slph and pre-heating temperature equal to 545°C.

Figure 11 - Operating maps in the plane pressure/flow rate for F (▲), P1 (●) and P2 (■) monoliths. O_2 = 10%; CH_4 = 3.7%; N_2 = balance.

Tables captions

Table 1 - Features of the fully and partially coated monoliths

Table 2 - Operating conditions adopted for experimental tests

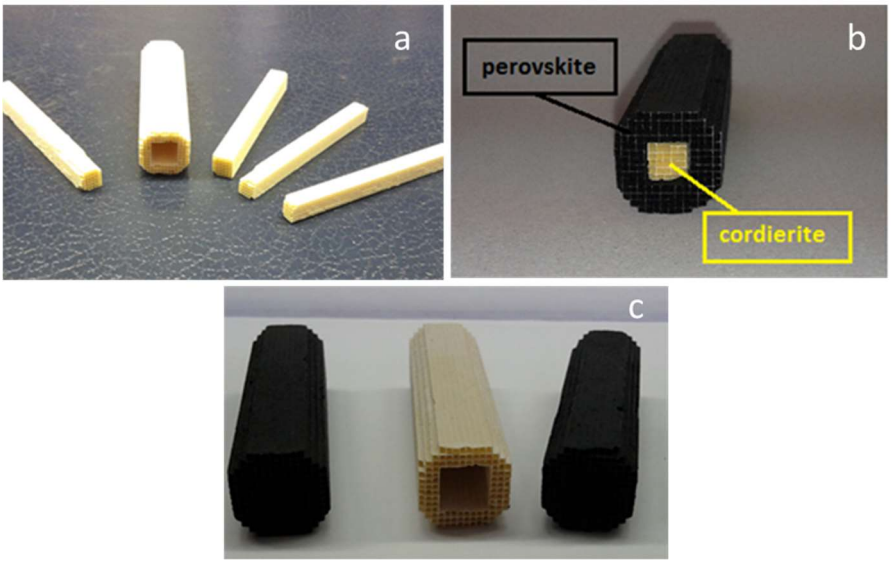

Figure 1

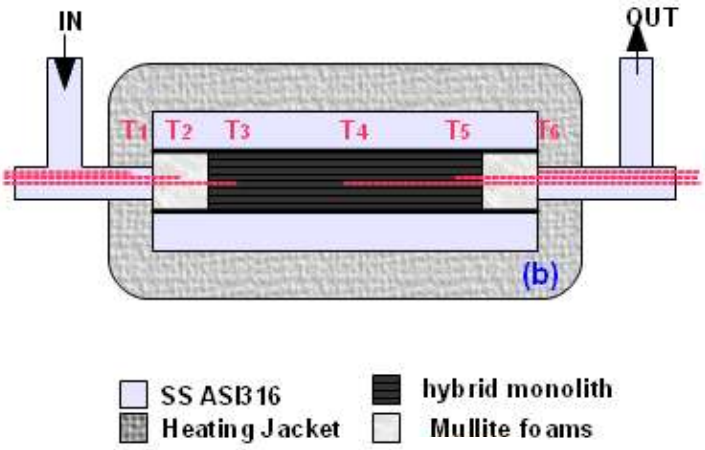

Figure 2

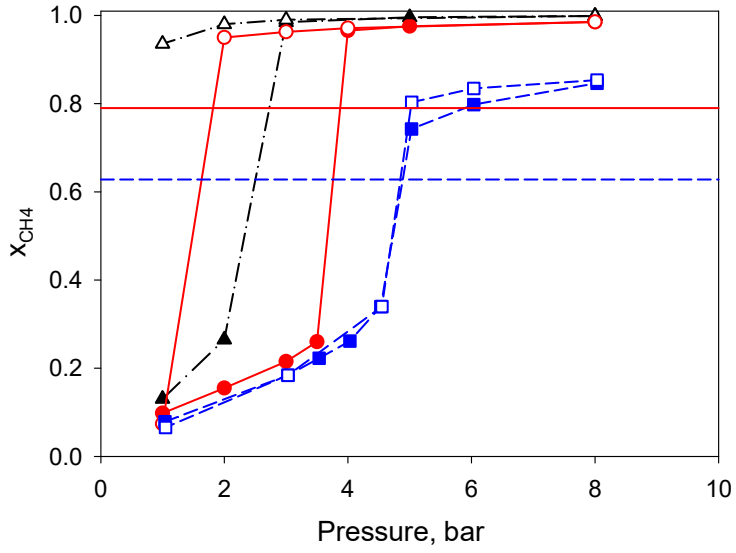

Figure 3

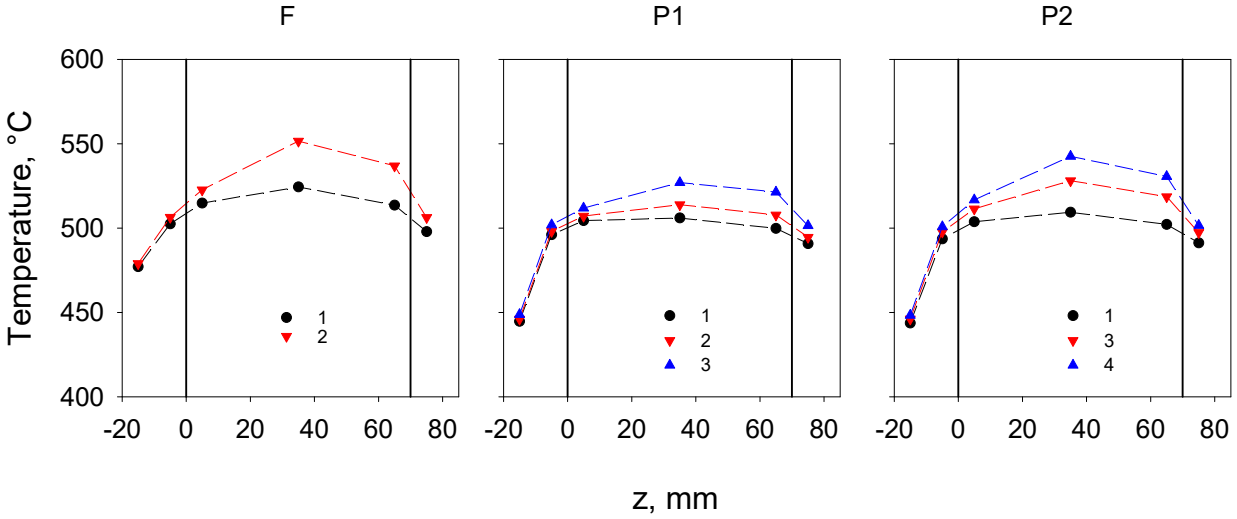

Figure 4

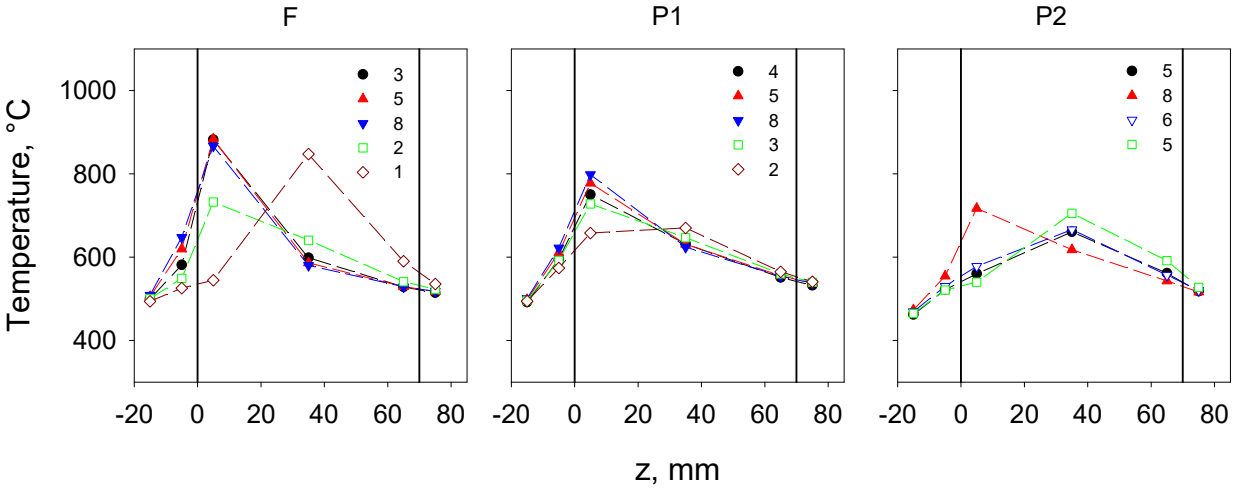

Figure 5

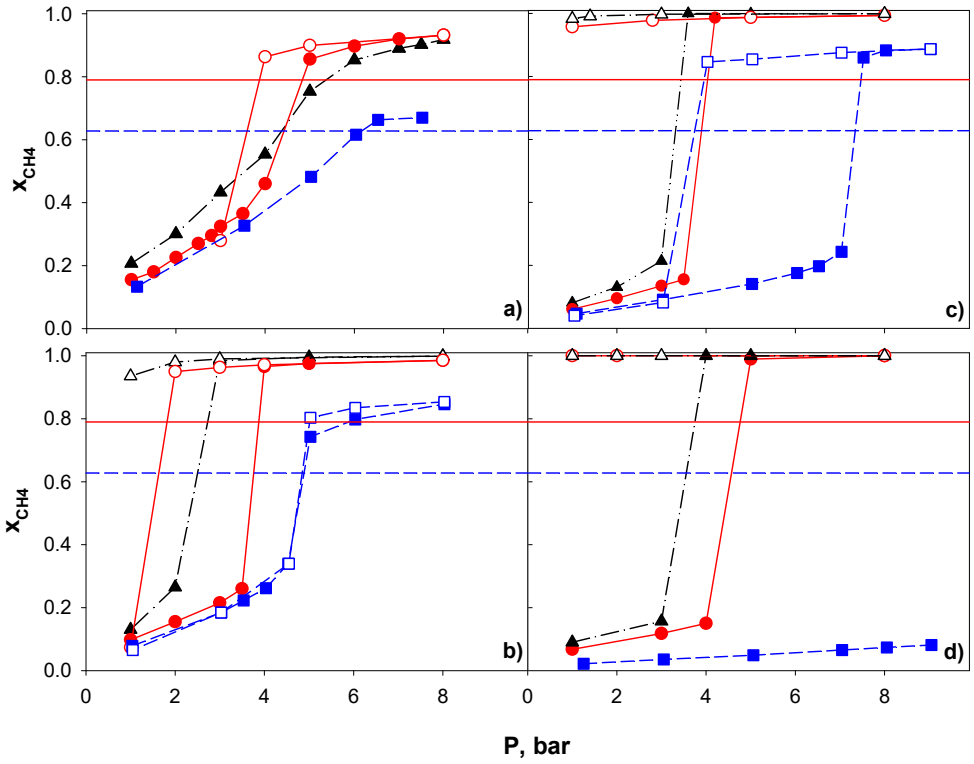

Figure 6

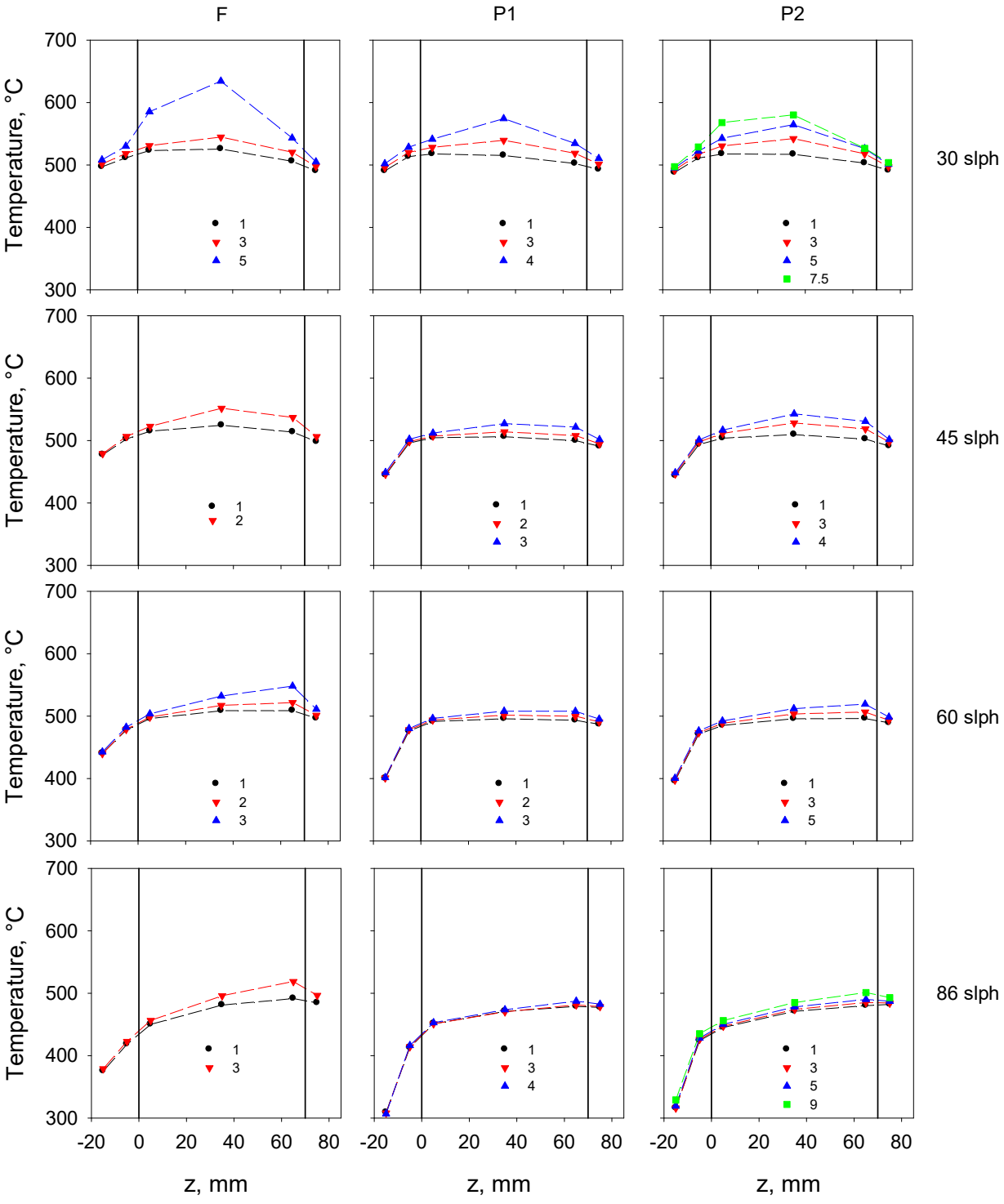

Figure 7

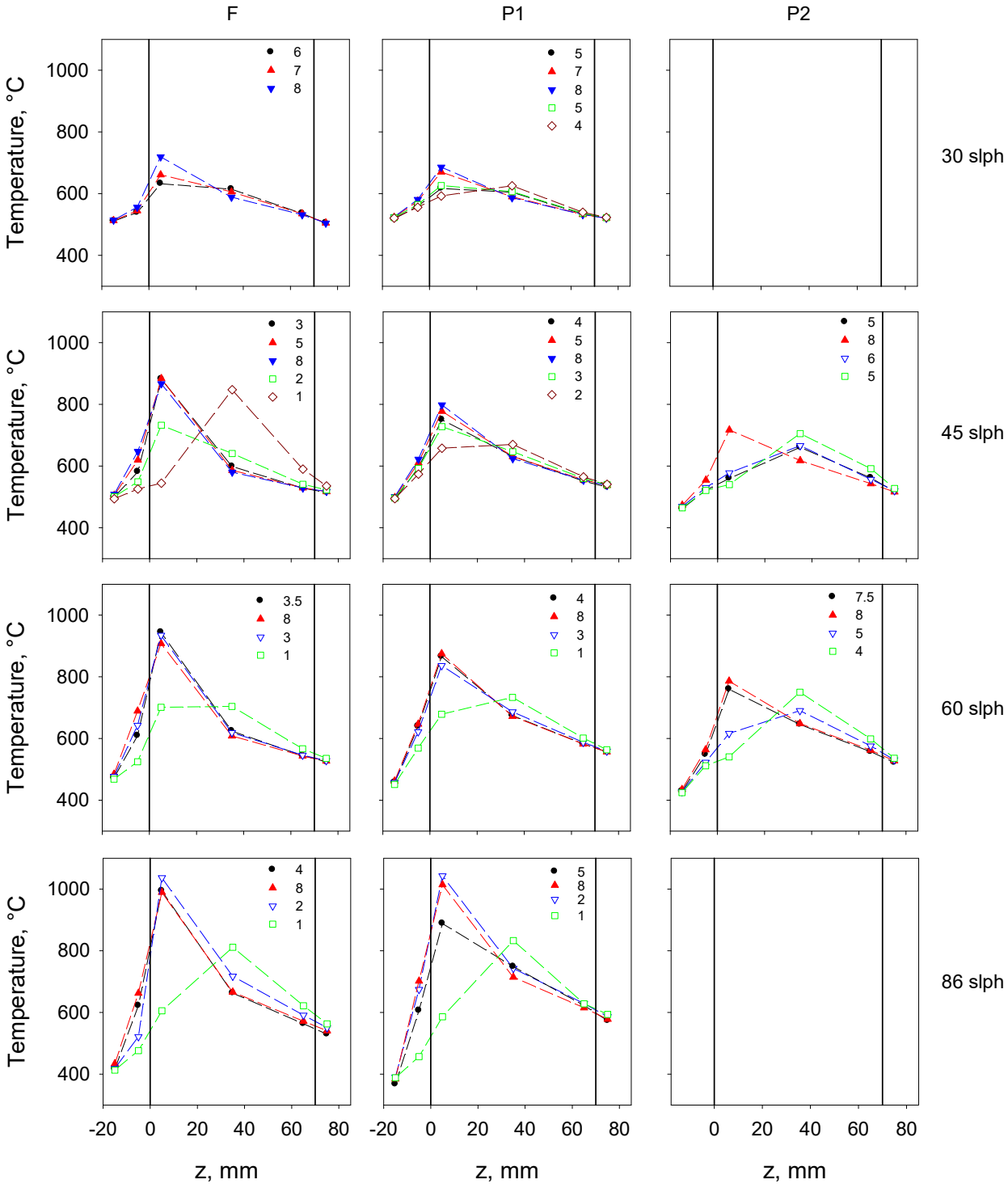
F
P1
P2
Temperature, °C
1000
800
600
400
6
7
8
5
7
8
5
4
30 slph
3
5
8
2
1
4
5
8
3
2
5
8
6
5
45 slph
3.5
8
3
1
4
8
3
1
7.5
8
5
4
60 slph
4
8
2
1
5
8
2
1
86 slph
-20
0
20
40
60
80
z, mm

Figure 8

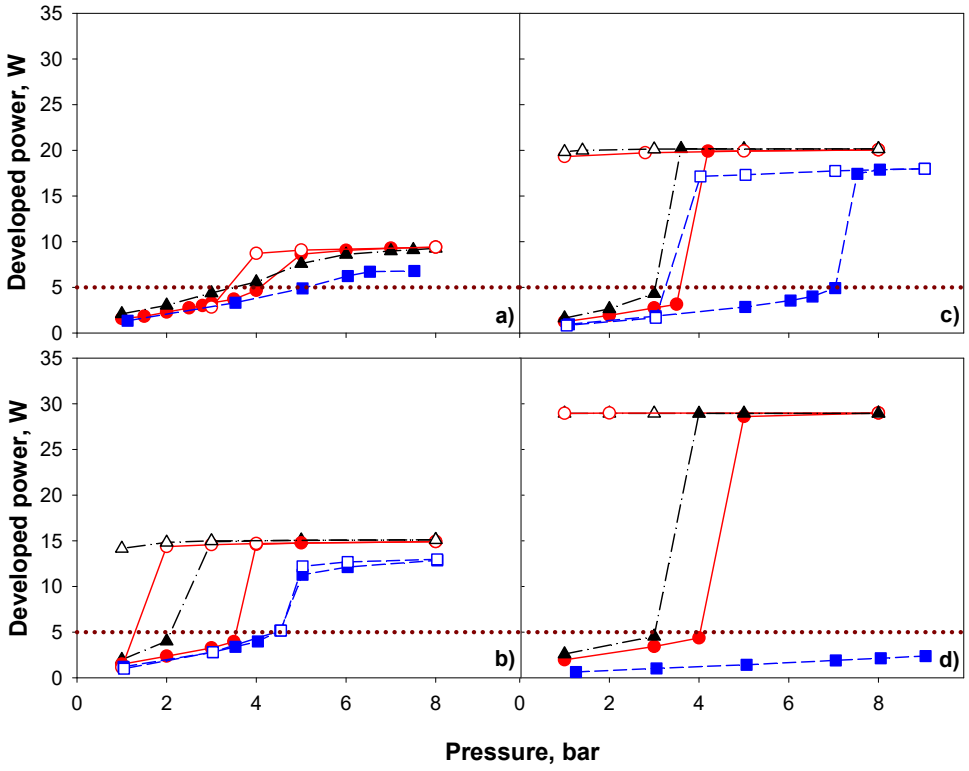

Figure 9

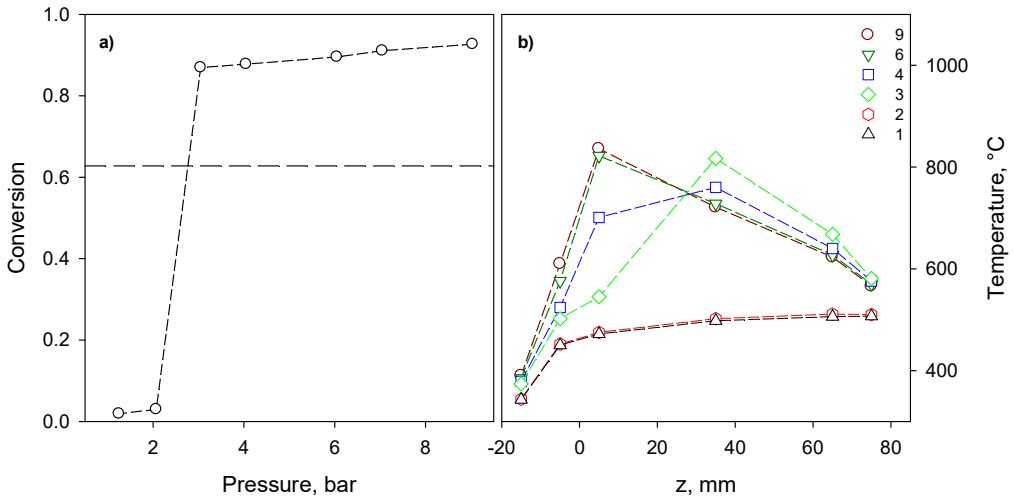

Figure 10

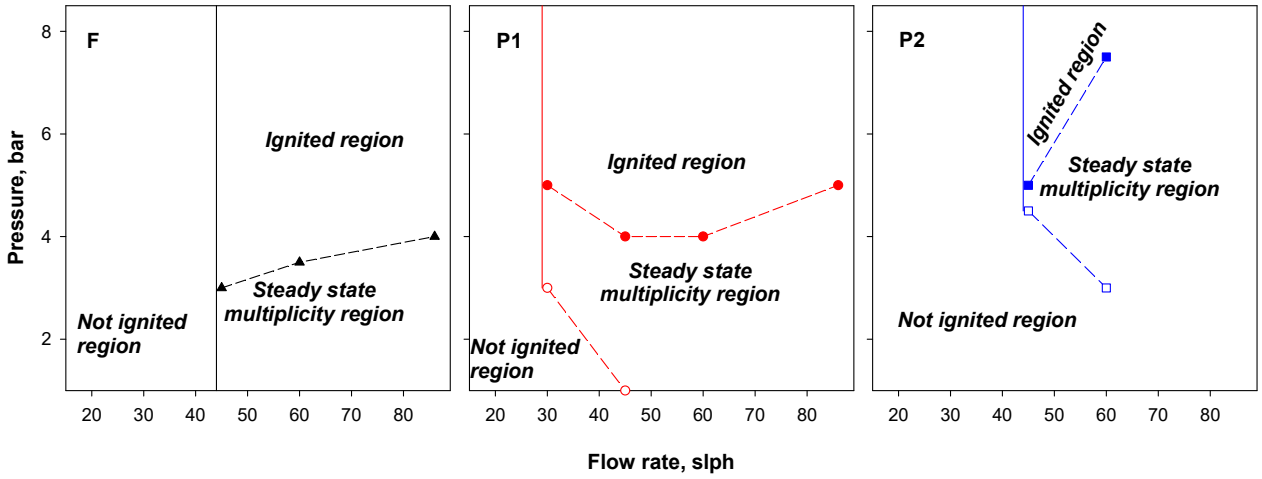
F
P1
P2
Pressure, bar
Flow rate, slph
Ignited region
Steady state multiplicity region
Not ignited region
Ignited region
Steady state multiplicity region
Not ignited region
Ignited region
Steady state multiplicity region
Not ignited region

Figure 11

Table 1

Monolith	D, mm	L, mm	Cell density, cpsi	Total channels	Coated channels	Coated fraction	Catalyst weight, g
F	12	50	900	172	172	1	1.83
P1					136	0.79	1.36
P2					108	0.63	1.11

Table 2

Pre-heating temperature, °C	520[a,b]
CH_4, %	3.7
O_2, %	10.0
N_2, %	balance
Thermal power, W_{th}	10-30
Q_{TOT}, slph	30-86
Re^{IN} [c], @STP	5-150
GHSV [d], @ STP, h^{-1}	$7.2 \cdot 10^3$-$2.1 \cdot 10^4$
P, bar	1-9

[a] *measured at the entrance of the monoliths in the absence of flow*
[b] *unless otherwise specified*
[c] *calculated inside the channels*
[d] *calculated by using monolith void volume*